

This is a repository copy of *Malat1 regulates female Th2 cell cytokine expression through controlling early differentiation and response to IL-2*.

White Rose Research Online URL for this paper:

<https://eprints.whiterose.ac.uk/id/eprint/231131/>

Version: Published Version

Article:

Gwynne, Mags, West, Katie A, van Dongen, Stijn et al. (6 more authors) (2025) Malat1 regulates female Th2 cell cytokine expression through controlling early differentiation and response to IL-2. *Journal of Immunology*. vkaf177. ISSN: 1550-6606

<https://doi.org/10.1093/jimmun/vkaf177>

Reuse

This article is distributed under the terms of the Creative Commons Attribution (CC BY) licence. This licence allows you to distribute, remix, tweak, and build upon the work, even commercially, as long as you credit the authors for the original work. More information and the full terms of the licence here:

<https://creativecommons.org/licenses/>

Takedown

If you consider content in White Rose Research Online to be in breach of UK law, please notify us by emailing eprints@whiterose.ac.uk including the URL of the record and the reason for the withdrawal request.

Malat1 regulates female Th2 cell cytokine expression through controlling early differentiation and response to IL-2

Mags Gwynne, Katie A West, Stijn van Dongen, Ioannis Kourtzelis, Dawn Coverley, Sarah A Teichmann, Kylie R James, James P Hewitson, Dimitris Lagos



STING Ligands

Enhance Delivery Efficiency.
Adapt to Tumor Diversity.
Eliminate Toxicity.

[Learn More](#)

InvivoGen

The advertisement features a blue gradient background on the left with white text. On the right, there is a photograph of two stingrays resting on white sand under a clear blue sky. The InvivoGen logo is positioned vertically on the far right in white text on a red background.

results in stronger immune responses through suppression of interleukin (IL)-10 expression in mouse models of type 1 immunity to parasitic infection, including visceral leishmaniasis and malaria. In humans, *Malat1* downregulation is a hallmark of proliferative CD4⁺ and CD8⁺ T cells.²¹ Others have linked *Malat1* to CD4⁺ T cell function, particularly in Th17 cells,^{22,23} and to CD8⁺ T cell function.²⁴

In our previous report, which focused on Th1 cells, we showed that *Malat1* loss also affected IL-10 expression in in vitro differentiated Th2 cells.²⁰ Although expressed by all effector Th cells, IL-10 expression is highest in Th2 cells,²⁵ which we have also shown previously.²⁰ However, the role of *Malat1* in Th2 cell differentiation and function remain underexplored. Here, we aimed to test how loss of *Malat1* affects Th2 differentiation in vitro and in an in vivo model of type 2 inflammation, *Schistosoma mansoni* egg injection.^{26,27} We report that *Malat1* deficiency leads to impaired Th2 differentiation with widespread effects across the transcriptome and a notable suppression of IL-10 expression only observed in female-derived Th2 cells. Although some effects caused by *Malat1* deficiency are shared between male- and female-derived CD4⁺ T cells, *Malat1* loss has more profound effects on female Th2 cells. This is due to a female-specific impaired regulation of an early differentiation interferon-stimulated gene (ISG) expression program, suppression of IL-2 receptor (IL2R) expression in *Malat1*^{-/-} cells, and increased sensitivity of female cells to IL-2-driven cytokine production.

Materials and methods

Animals and ethics

Animal care and experimental procedures were regulated under the Animals (Scientific Procedures) Act 1986 (revised under European Directive 2010/63/EU) and were performed under UK Home Office License (project license number PP0841992 for breeding and PP9423191 for *S. mansoni* egg injections) with approval from the University of York Animal Welfare and Ethical Review Body. Animal experiments conformed to Animal Research: Reporting of In Vivo Experiments guidelines.²⁸

S. mansoni egg injection

C57BL/6 CD45.2 wild-type (WT) mice were obtained from Charles River Laboratories. *Malat1*^{-/-} mice (complete knockouts) were obtained from the Riken Institute.¹⁸ All mice were bred in-house, maintained under specific pathogen-free conditions, and used at 6 to 12 wk of age. Schistosome eggs were recovered from the livers of C57BL/6 mice at week 7 postinfection following exposure to 100 *S. mansoni* cercariae. Cercariae were obtained from schistosome-infected *Biomphalaria glabrata* snails provided by the Barrett Centre for Helminth Control (Aberystwyth University, United Kingdom). Livers were digested overnight at 37°C with shaking with 0.2 U/mL collagenase D (Roche) in the presence of 5,000 U/mL polymyxin B (Merck). Eggs were purified by centrifugation through 10 mL Percoll (GE Healthcare)/20 mL 0.25M sucrose (450 g, 5 min, room temperature), washed in phosphate-buffered saline (PBS), and stored at -20°C before usage. A total of 5,000 dead *S. mansoni* eggs in 200 µL PBS were delivered via intraperitoneal injection into mice. Two weeks later, the mice were intravenously challenged with another 5,000 eggs in 200 µL PBS. After another week, the mice were sacrificed and the lungs and spleen were extracted and processed. Lungs were digested with 0.4 U/mL Liberase TL

(Roche) and 80 U/mL DNase I type IV in HBSS (both Sigma-Aldrich) for 45 min at 37°C. Enzyme activity was inhibited with 10 mM EDTA (pH 7.5), and single-cell suspensions were created with 100 µm nylon filters (Falcon) in complete RPMI 1640 (Thermo Fisher Scientific) supplemented with 10% heat-inactivated fetal calf serum (HyClone), 100 U/mL penicillin, 100 µg/mL streptomycin, and 2 mM l-glutamine (all Thermo Fisher Scientific), then cleaned via Percoll gradient and 3 mL ACK red blood cell lysis buffer. Spleen single-cell suspensions were generated in the same manner and only passed through a 70 µm filter and treated with 3 mL ACK buffer.

In vitro Th2 differentiation and *Malat1* knockdown

Spleens and axillary, brachial, mesenteric, and inguinal lymph nodes of WT or *Malat1*^{-/-} mice were extracted and homogenized through a 70 µm filter in RPMI 1640. Resulting cell pellets were then treated with 3 mL ACK lysis buffer. Naïve CD4⁺ T cells were then purified via MACS column isolation (Miltenyi Naïve CD4⁺ T Cell Isolation Kit, mouse, catalog number 130-104-453), normally resulting in purity of ~95%. For Th2 polarization, purified naïve CD4⁺ T cells (500,000 cells per well) were stimulated with 10 µg/mL plate-bound anti-CD3ε (clone 145-2C11) and 4 µg/mL soluble anti-CD28 (37.51) in RPMI 1640 in flat-bottom 96-well plates in the presence of 25 ng/mL mouse recombinant IL-4 and 5 µg/mL anti-IFNγ (XMG1.2). Anti-CD3/anti-CD28-dependent activation (4 d) was followed by rest in 10 U/mL human recombinant IL-2 for 2 d. Titrations of anti-CD3ε antibody or recombinant IL-2 were performed as indicated. Recombinant cytokines were from PeproTech. For *Malat1* knockdown experiments, control or *Malat1*-targeting antisense oligonucleotide GapmeRs were from QIAGEN (LG00000002-DDA and LG00000008-DDA, respectively) and were added to naïve CD4⁺ T cells on day 0, or differentiating Th2 cells on day 4, at a final concentration of 100 nM. For IL-10 receptor (IL10R) blockade experiments, CD4⁺ T cells were treated either with anti-IL10R (clone: 1B1.3A; Bio X Cell) or rat IgG at 10 µg/mL as a control, at both days 0 and 4. For interferon β (IFNβ) treatment experiments, cells were treated with 5,000 U/mL mouse IFNβ (CYT-651; Prospec), at day 0.

Flow cytometry

For flow cytometry analysis, single-cell suspensions were generated. For live/dead discrimination, cells were washed twice in PBS, then stained with Zombie Aqua (BioLegend) in PBS before resuspension in FACS (fluorescence-activated cell sorting) buffer (PBS containing 0.5% bovine serum albumin and 0.05% azide). Fc receptors were blocked with 100 µg/mL rat IgG (Sigma-Aldrich) for 10 min at 4°C before surface staining for 30 min at 4°C. The following anti-mouse antibodies from BioLegend were used: CD45.2 BV786 (clone 104); TCRβ PE-Cy7 (H57-597); CD19 APC-Cy7 (6D5); MHC class II (MHCII) Alexa Fluor 700 (M5/114.15.2); Ly-6G APC-Cy7 (1A8); Ly6C BV605 (HK1.4); CD64 PE (X54-5/7.1); CD11b Pacific Blue (M1/70); CD44 FITC (IM7); CD62L PE (MEL-14); CD8α PB (53-6.7); CD4 PerCP/Cy5.5 (RM4-5); IFN-γ FITC (XMG1.2); IL-10 PE (JES5-16E3); IL-4 PE-Dazzle or APC (11B11); CD25 (IL-2Ra) PerCP-Cy5.5 or APC (PC6.1); CD69 APC (H1.2F3); CD132 (IL-2Rg) PE (TUGm2); GATA3 PE-Dazzle 594 (16E10A23); and IFNAR1-PE (MAR1-5A3) and streptavidin PE-Cy7. These

were used in combination with antibodies SiglecF PerCP-eFluor 710 (1RNM44N), iNOS PE-eFluor 610 (CXNET), and goat anti-rabbit A647 from Thermo Fisher Scientific, biotinylated Ym1 from R&D systems, anti-murine RELM α from PeproTech, and IL-13 PB (eBio13A) from eBioscience. To measure intracellular cytokines in T cells following ex vivo stimulation, cells were first stimulated in complete RPMI 1640 for 4 h at 37 °C with 500 ng/mL PMA, 1 μ g/mL ionomycin, and 10 μ g/mL brefeldin A (all Sigma-Aldrich). For all intracellular cytokine staining, surface-stained cells were fixed and permeabilized (20 min at 4 °C) using Fixation/Permeabilization Solution before washes in Perm/Wash buffer (both BD Biosciences). Cells were then stained with intracellular antibodies as above except in Perm/Wash buffer. For transcription factor staining, surface stained cells were fixed and permeabilized (1 h or overnight at 4 °C) using the FoxP3 Fixation/Permeabilization solution before washes in 1 \times Permeabilization Buffer (eBioscience). Cells were stained with intracellular antibodies as previously except in Permeabilization Buffer. Appropriate isotype or fluorescence-minus-one controls were used to draw gates for populations of interest. Events were acquired on an LSRFortessa (BD Biosciences) with analysis by FlowJo v9.6 (TreeStar) or a Cytotflex LX (Beckman Coulter) before analysis with CytExpert.

RNA extraction, complementary DNA synthesis, and quantitative reverse-transcription polymerase chain reaction (qRT-PCR)

RNA was extracted from purified cell populations using QIAzol and miRNeasy RNA extraction kits (QIAGEN) according to manufacturer's instructions. For mRNA transcripts, reverse transcriptions were carried out with Superscript III (Thermo Fisher Scientific) and random hexamer primers (Promega) and measured with Fast SYBR Green Master Mix (Thermo Fisher Scientific). Quantitative polymerase chain reaction (PCR) was performed using a StepOnePlus Real Time PCR System or a QuantStudio 3 (both Thermo Fisher Scientific), and relative transcript levels were determined using the $\Delta\Delta C_t$ method. The primers used for the study are shown in [Table S1](#).

RNA sequencing and analysis

We used short-read (Illumina) RNA sequencing (RNAseq) to compare naïve CD4⁺ T cells and in vitro differentiated Th2 cells from female and male WT and *Malat1*^{-/-} mice. Pooled complementary DNA (cDNA) libraries were sequenced on lane of an Illumina NovaSeq 6000 S4 flow-cell at 100PE. The raw sequencing reads were aligned to the mouse genome version Ensembl GRCm38.92 with STAR 2.5.4a. We sequenced 4 replicates per condition. Samples with assigned sequencing reads lower than 500,000 were removed from downstream analysis. Of the remaining samples (n = 4 for all *Malat1*^{-/-} samples and WT male Th2, n = 3 for WT female and male naïve CD4⁺ T cells and WT female Th2), we obtained an average of 65 million reads per sample (range: 52–91 million). Analysis was performed in RStudio (version 1.4.1106) with R (version 4.1; R Foundation for Statistical Computing). Data were normalized (“calcNormFactors” and “estimateDisp” functions of edgeR (version 3.14.0)) and a quasi-likelihood negative binomial generalized log-linear model (“glmQLFit” and “glmQLFTest” functions with coefficient = 2) was used

to determine differentially expressed genes. Adjusted *P* values were calculated using the Benjamini-Hochberg method.

We used Oxford Nanopore Technologies (ONT) long-read RNAseq to compare naïve CD4⁺ T cells and cells after 2 d of in vitro differentiation from female WT and *Malat1*^{-/-} mice (n=4 per group). Full length cDNA libraries were prepared using the ONT cDNA-PCR Sequencing V14 - Barcoding kit (SQK-PCB114.24). Briefly, cDNA RT adapters were ligated to 3' ends (polyA tails) of transcripts prior to strand switching cDNA synthesis and a 13-cycle PCR reaction with barcoded primers, labeling each cDNA sample with a unique DNA barcode. Barcoded cDNAs were pooled at equimolar ratios before final adapter ligation and sequencing on R10.4.1 flow cells in ONT PromethION sequencer (8 samples per flow cell). Live superaccuracy basecalling and barcode demultiplexing were performed in MinKNOW software (version 24.06.10; ONT) at the time of the run. We acquired 0.745 to 1.121 million reads per sample, with 604 to 840 bases mean read length. Demultiplexed reads were analyzed through the workflow Transcriptomes from Epi2Me application, specifically designed by ONT. The workflow generates differential gene expression data (with edgeR), as well as differential transcript usage (DTU) data (with DEXSeq), using a reference transcriptome. The Viking cluster, provided by the University of York, was used for the analyses.

Statistics

Experiments were typically performed in 2 to 3 independent replicates in groups of 3 to 5 mice per condition and replicate. Statistical analyses were carried out as indicated with Prism 5 (GraphPad Software). Two-way comparisons used paired or unpaired *t* tests as indicated, and multiple comparisons used 1-way analysis of variance, followed by Sidak's multiple comparisons test for comparison of samples with biological relevance (e.g. WT female with *Malat1*^{-/-} female, WT male with *Malat1*^{-/-} male, WT female with WT male). Confidence levels were set to 0.05 for significance. In merged data where $n > 9$, consensus between Anderson-Darling, Shapiro-Wilk, and D'Agostino and Pearson tests were used to determine normality. If all samples were normally distributed 1-way analysis of variance was performed as described. If 1 or more samples did not follow a normal distribution, a Kruskal-Wallis test followed by Dunn's multiple comparison test were performed to identify significance, with confidence levels of 0.05. *P* values are displayed as asterisks representing *P* value classification, unless the results are borderline nonsignificant, in which case the *P* value is shown.

Results

Malat1 loss impairs in vitro Th2 differentiation of CD4⁺ T cells from female mice

We first assessed the effect of *Malat1* deletion on Th2 differentiation in vitro in response to stimulation with anti-CD3 and anti-CD28 antibodies in the presence of recombinant IL-4 and anti-IFN γ antibody for 4 d, followed by IL-2 treatment for 2 d. This protocol allowed us to dissect potential effects on naïve CD4 $^{+}$ T cell activation (0–24 h), early differentiation (2–4 d), and terminal differentiation in response to exogenous IL-2 (Fig. 1A). Following in vitro differentiation of naïve CD4 $^{+}$ T cells from female mice to Th2 cells, *Malat1* $^{-/-}$ cells displayed significantly lower percentages of IL-10 $^{+}$ and IL-4 $^{+}$ /IL-10 $^{+}$ cells at day 6 of differentiation, with no

differences in IL-4⁺/IL-10⁻ cells, and no differences at day 4 (Fig. 1B–F; Fig. S1A). This decrease in cytokine expression was not observed from cells derived from male mice. Under

these conditions, differentiation of WT CD4⁺ T cells from male mice was less efficient compared with female WT cells, and *Malat1* deletion did not affect this further (Fig. 1B–F).

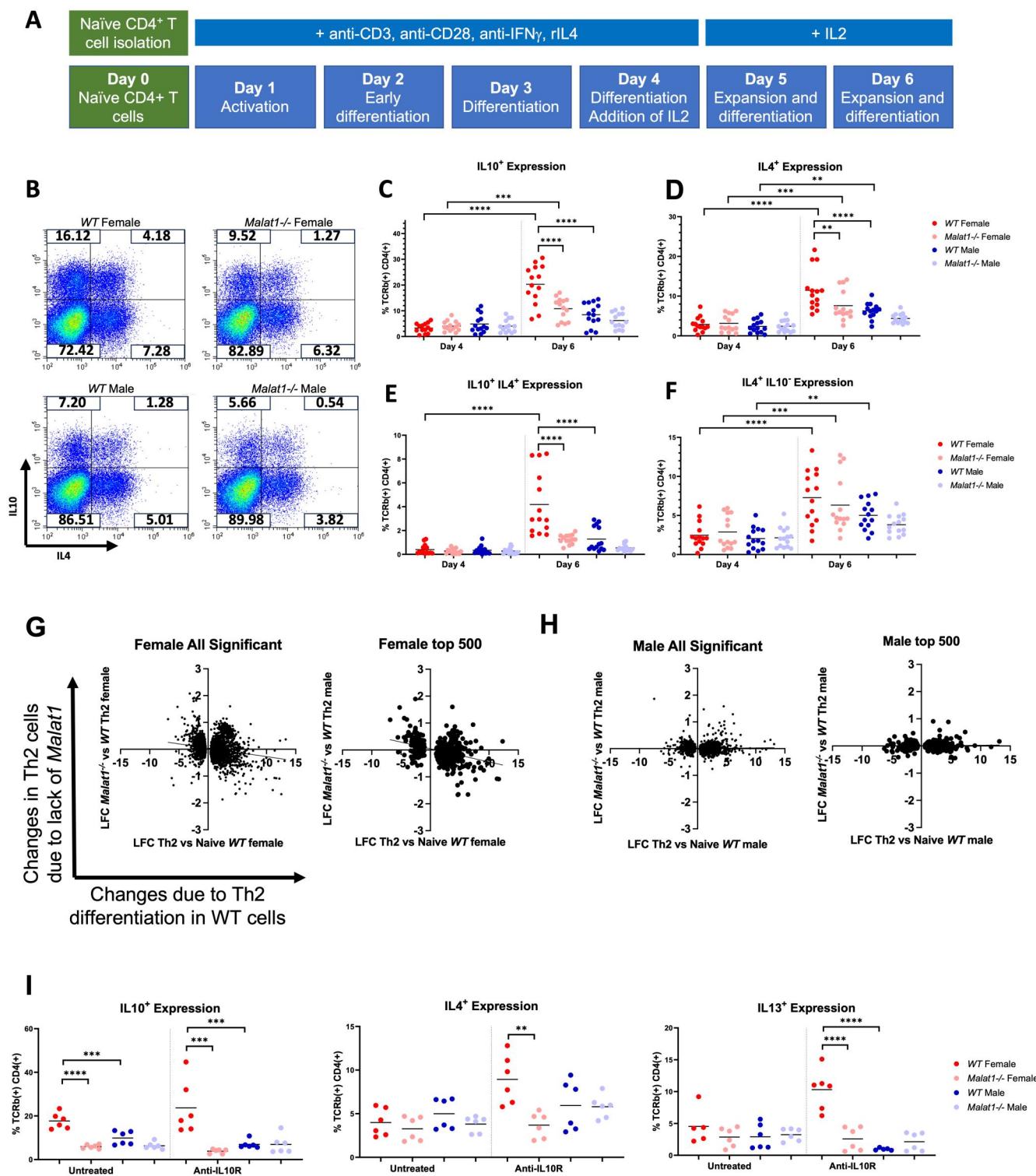


Figure 1. *Malat1* loss impairs in vitro Th2 differentiation only in female cells. (A) Schematic of in vitro Th2 differentiation protocol. (B) Representative FACS plots of IL-10 and IL-4 expression in WT and *Malat1*^{-/-} female and male in vitro differentiated Th2 cells (day 6). (C) Percentage of IL-10⁺ live TCRb⁺ CD4⁺ in vitro differentiated Th2 cells derived from female and male mice at day 4 (prior to IL-2 addition) and day 6 (experimental endpoint). Levels determined by intracellular cytokine staining (n = 14 per condition). (D) As in panel C, but for IL-4⁺ live TCRb⁺ CD4⁺ cells. (E) As in panel C, but for IL-4⁺/IL-10⁺ live TCRb⁺ CD4⁺ cells. (F) As in panel C, but for IL-4⁺/IL-10⁻ live TCRb⁺ CD4⁺ cells. (G) LFC in gene expression between WT female naive and in vitro differentiated Th2 cells against LFC in gene expression between WT and *Malat1*^{-/-} female in vitro differentiated Th2 cells. Data shown for all or the top 500 DEGs between Th2 and naive CD4⁺ T cells from WT female mice. (H) As in panel G, but for cells derived from male mice. (I) Percentage of IL-10⁺, IL-4⁺ or IL-13⁺ live TCRb⁺ CD4⁺ in vitro differentiated Th2 cells derived from WT or *Malat1*^{-/-} female and male mice at day 6, with or without treatment with 10 µg/mL of anti-IL10R antibody. Levels determined by intracellular cytokine staining (n = 6 per condition). ***P* ≤ 0.01, ****P* ≤ 0.001, *****P* ≤ 0.0001.

RNAseq analysis of WT and *Malat1*^{-/-} naïve CD4⁺ T cells and in vitro differentiated Th2 cells revealed only a small number of genes were statistically significantly differentially expressed between WT and *Malat1*^{-/-} cells (Table S2). As shown previously,²⁰ IL-10 levels were suppressed in *Malat1*^{-/-} Th2 cells compared with WT controls (log₂ fold change [LFC] = -0.882, *P* = 0.034, for female-derived cells; and LFC = 0.03, *P* = 0.932 for male-derived cells), although this did not reach significance after multiple testing correction. This was further confirmed by quantitative reverse-transcription polymerase chain reaction (qRT-PCR) for the sequenced samples (Fig. S1B), suggesting that this bulk RNAseq analysis provided a conservative representation of the effect of *Malat1* deficiency on Th2 gene expression. Focusing on genes that were differentially expressed between Th2 and naïve CD4⁺ T cells from WT mice (Th2-differentiation associated genes), we observed a transcriptome-wide blunting of Th2 gene expression upon *Malat1* loss in female but not male cells (Fig. 1G, H; Tables S3–S5). Analysis of all (false discovery rate [FDR] < 0.001) or the top (by FDR) 500 differentially expressed genes (DEGs) between WT Th2 and naïve CD4⁺ T cells demonstrated that most genes that were upregulated during WT Th2 differentiation were overall expressed at lower levels when comparing *Malat1*^{-/-} Th2 cells with WT Th2 cells, and conversely, genes that were suppressed upon WT Th2 differentiation were overall more highly expressed in *Malat1*^{-/-} Th2 cells (Fig. 1G; Tables S3–S5). This transcriptome-wide trend was not observed in male cells (Fig. 1H). Taking a stricter threshold for DEGs between Th2 and naïve CD4⁺ T cells from female mice (FDR < 0.001 and absolute LFC > 2), we found 524 Th2 differentiation-associated DEGs in both WT and *Malat1*^{-/-}, 469 DEGs only in WT, and 139 DEGs only in *Malat1*^{-/-} Th2 cells. We noted that common and WT only Th2 DEGs were mainly upregulated, whereas *Malat1*^{-/-} only Th2 DEGs were mainly downregulated (Fig. S1C, D and Tables S3–S5). Furthermore, when looking at common DEGs, we found that the vast majority of upregulated genes showed a smaller LFC in *Malat1*^{-/-} Th2 cells compared with WT (Fig. S1E). To distinguish the effect of *Malat1* from that of IL-10, we blocked the IL10R between days 4 and 6 of differentiation. As previous, in control conditions, the effect of *Malat1* on IL-4 and IL-13 effector Th2 cytokines was modest. However, upon blockade of IL10R, *Malat1* loss resulted in dramatic and statistically significant decrease in IL-4 and IL-13 expression in female-derived Th2 cells, with no effect on male-derived cells (Fig. 1I). Overall, these results indicated that *Malat1* loss impairs Th2 differentiation of female- but not male-derived naïve CD4⁺ T cells, characterized by suppression of IL-10 expression and an impairment of the Th2 gene expression program.

The effect of *Malat1* depletion on IL-10 expression is independent of activation strength and occurs during the early stages of differentiation

We next tested whether *Malat1* deficiency affected Th2 polarization under weaker activation conditions. We found that *Malat1*^{-/-} cells displayed lower IL-10 expression under suboptimal differentiation conditions, whereas IL-4 levels were not statistically significantly different (Fig. 2A, B; Fig. S2A, B). Of note, at lower activation levels there were no differences in IL-10 expression between in vitro Th2 differentiation of male and female cells. This indicated that *Malat1*

deficiency can affect Th2 cytokine expression independently of activation strength. Under suboptimal differentiation conditions, IL10R blockade did not enhance the effect of *Malat1* deficiency on IL-4 or IL-13 expression, potentially due to the low cytokine expression levels under these conditions (Fig. S2C).

We next tested whether *Malat1* knockdown rather than genetic deletion had a sex-specific effect on Th2 differentiation. As described previously,²⁰ we used GapmeR oligonucleotides to suppress *Malat1* expression (Fig. S2D). Although Th2 cells express lower *Malat1* levels than naïve CD4⁺ T cells (as shown in Hewitson et al. and Fig. S2E),²⁰ we found that *Malat1* levels increase between days 4 and 6 of differentiation, upon cessation of CD3 activation and addition of exogenous IL-2 (Fig. 2C). As for cytokine expression (Fig. 2A, B), the increase in *Malat1* levels in response to IL-2 (days 4 to 6) was more profound in female cells. We note that there were no differences in *Malat1* expression between WT male and female naïve (Fig. S2E) or differentiating (day 4) (Fig. 2C) CD4⁺ T cells prior to IL-2 stimulation.

Based on the observation that *Malat1* deficiency impaired cytokine induction between days 4 and 6 (Fig. 1C–F), we knocked down *Malat1* on day 0, or by adding GapmeRs on day 4, at the same time with exogenous IL-2 stimulation. *Malat1* knockdown reduced IL-10 expression in female Th2 cells only if GapmeRs were added to naïve CD4⁺ T cells, but not when added concurrently with exogenous IL-2 stimulation. No effects on cytokine expression were observed upon *Malat1* knockdown in male cells (Fig. 2D). Partial knockdown of *Malat1* in cells from female mice did not affect IL-4 expression (Fig. S2F). As in the case of *Malat1*^{-/-} cells, IL10R blockade enhanced the effect of *Malat1* GapmeR-mediated knockdown on IL-4 (Fig. 2E). This was not observed for IL-13, potentially due to low IL-13 expression under these conditions (Fig. 2E). We noticed that treatment with nontargeting control GapmeRs consistently resulted in lower IL-13 cytokine expression in Th2 cells (compare Fig. 2E with Fig. 1I). Overall, this demonstrated that the effect of *Malat1* on Th2 cytokine expression required its activity during the early differentiation stages.

Malat1 loss alters the kinetics of naïve CD4⁺ T cell activation and impairs early Th2 differentiation

Based on the previous, we tested the effect of *Malat1* deletion on the early stages of Th2 differentiation. First, we studied the first 24 h of naïve CD4⁺ T cell activation by measuring levels of T cell early activation marker CD69 (Fig. S3A). As expected, *Malat1* levels were suppressed within 24 h in both male and female WT mice (Fig. S3B). In female cells, we found that compared with WT cells CD69 protein expression was higher in *Malat1*^{-/-} cells at 3 h postactivation, the difference reaching statistical significance at 7 h postactivation. However, CD69 expression was significantly lower in *Malat1*^{-/-} cells at 24 h (Fig. 3A). At the transcript level, *Cd69* levels peaked at 3 h postactivation, with significantly higher levels in *Malat1*^{-/-} cells (Fig. S3C). In male cells, we did not observe any statistically significant differences between WT and *Malat1*^{-/-} cells, although we noted that male WT cells showed statistically significant higher CD69 levels compared with female counterparts at 3 h post activation (Fig. 3A). We also measured levels of IL2Rα (CD25), which was induced upon activation but found no differences between genotypes or biological sexes (Fig. S3D).



To explore the consequences of the altered activation kinetics in female *Malat1*^{-/-} cells, we performed a daily time course (days 1–4), measuring transcript levels of key transcription factors (*Gata3*, *Maf*, and *Tbet*) and differentiation-associated genes (*Il2*, *Il2ra*, *Il2rg*). We focused on *Il2ra* and *Il2rg*, as the former is induced during differentiation and the latter is an X-linked gene, given the sex specificity of the observed effects. We noticed suppression for multiple of the measured transcripts in female *Malat1*^{-/-} differentiating cells, including *Il2*, *Il2ra*, *Il2rg*, and *Gata3* on days 2 and 3 of differentiation (Fig. 3B, C; Fig. S3E). These initial findings were confirmed in independent experiments for *Il2ra*, *Il2rg*, and *Gata3* on day 2 (Fig. 3D). We chose day 2 for the validation experiments as this was the earliest time point the suppression of the Th2 program was observed. In male *Malat1*^{-/-} cells, we observed higher variability and similar but non-statistically significant trends (Fig. 3D). GATA3 protein levels were suppressed in *Malat1*^{-/-} cells at day 2 of the differentiation in both male and female *Malat1*^{-/-} cells (Fig. 3E; Fig. S3F). At this point, we did not find any significant differences in the levels of the IL2R subunits (Fig. S3G). These results

To further explore the role of *Malat1* in early Th2 differentiation we performed long-read RNAseq of WT and *Malat1*^{-/-} naïve CD4⁺ T cells and differentiating cells at day 2 of differentiation. As *Malat1* has been suggested to be involved in regulation of mRNA splicing,¹⁴ we opted for long-read RNAseq to facilitate concurrent assessment of differential gene expression and DTU. As in the case of our short read RNAseq analysis, there were only few differences between WT and *Malat1*^{-/-} naïve CD4⁺ T cells (16 DEGs at FDR < 0.1) (Fig. S4A and Table S6). However, comparison of WT and *Malat1*^{-/-} cells on day 2 of differentiation revealed 239 DEGs, 199 of which were upregulated in *Malat1*^{-/-} cells (Fig. 4A; Table S7). Gene set enrichment analysis²⁹ revealed a profound overrepresentation of IFNα and IFNγ response gene signatures among the upregulated genes in *Malat1*^{-/-}

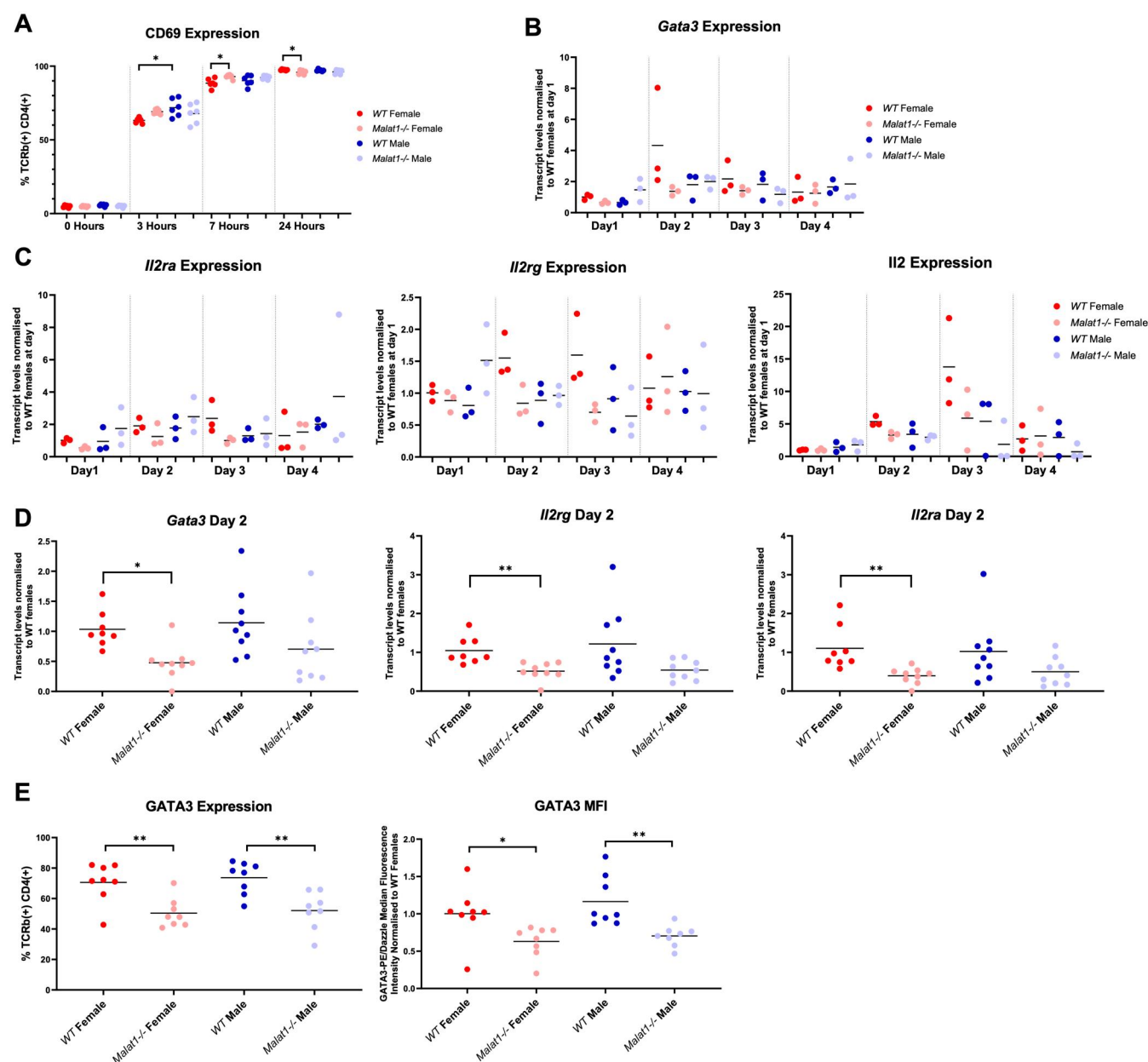


Figure 3. *Malat1* loss enhances naive CD4⁺ T cell activation and impairs early Th2 differentiation. (A) Percentage of CD69⁺ live TCRβ⁺ CD4⁺ WT or *Malat1*^{-/-} in vitro activated CD4⁺ T cells derived from female or male mice determined at 0, 3, 7, and 24 h postactivation. Levels determined by surface staining (n = 6). (B) *Gata3* mRNA levels at days 1, 2, 3, and 4 of Th2 differentiation determined by qRT-PCR (n = 3). Levels normalized to U6 and average levels of WT females at day 1. (C) *Il2ra*, *Il2rg*, and *Il2* mRNA levels at days 1, 2, 3 and 4 of Th2 differentiation determined by qRT-PCR (n = 3). Levels normalized to U6 and average levels of WT females at day 1. (D) *Il2ra*, *Il2rg*, and *Gata3* mRNA levels at day 2 of differentiation determined by qRT-PCR (n = 9). Levels normalized to U6 and average levels of WT females. (E) Percentage and median fluorescence intensity (MFI) of GATA3⁺ live TCRβ⁺ CD4⁺ WT or *Malat1*^{-/-} cells derived from female or male mice at day 2 of differentiation (n = 5 per condition). **P* ≤ 0.05, ***P* ≤ 0.01.

cells on day 2 (Fig. 4B), whereas enriched terms among downregulated genes, including hypoxia, only reached modest significance (Fig. S4B). We note that in agreement with our qRT-PCR analysis (Fig. 3D), trends toward downregulation were observed for *Il2ra* (LFC = -0.589) and *Gata3* (LFC = -0.401), but these did not reach statistical significance. The most prominent feature of *Malat1*^{-/-} cells, the upregulated IFN gene cluster (clusters identified by k-means clustering) (Fig. S4C and Table S8) included ISGs (e.g. *Ifit1bl1*, *Ifit3*, *Ifit1*, *Oas2*, and others) and transcription factors including *Irf7*, *Irf1*, and *Stat1* (Fig. 4C; Fig. S4C and Tables S7 and S8). Most of the day 2 *Malat1*-associated

DEGs were downregulated during differentiation of WT cells both when comparing day 2 with naïve cells (Fig. 4D) and when comparing WT Th2 and naïve CD4⁺ T cells using our short-read sequencing data (Fig. 4E). This was also the case specifically for the ISG module (Fig. S4D). As in the case of Th2 cells (Fig. 1G), *Malat1* deficiency had a transcriptome-wide effect by blunting changes in gene expression occurring in WT cells within the first 2 d of differentiation (Fig. S4E).

Validation of the long-read sequencing data by qRT-PCR for selected genes confirmed upregulation of *Ifit1bl1*, *Ifit3b*, *ligp1*, *Ifit1*, and *Irf7* (Fig. 4F). Upregulation trends for *Irf1* and *Stat1* did not reach statistical significance. Notably, no

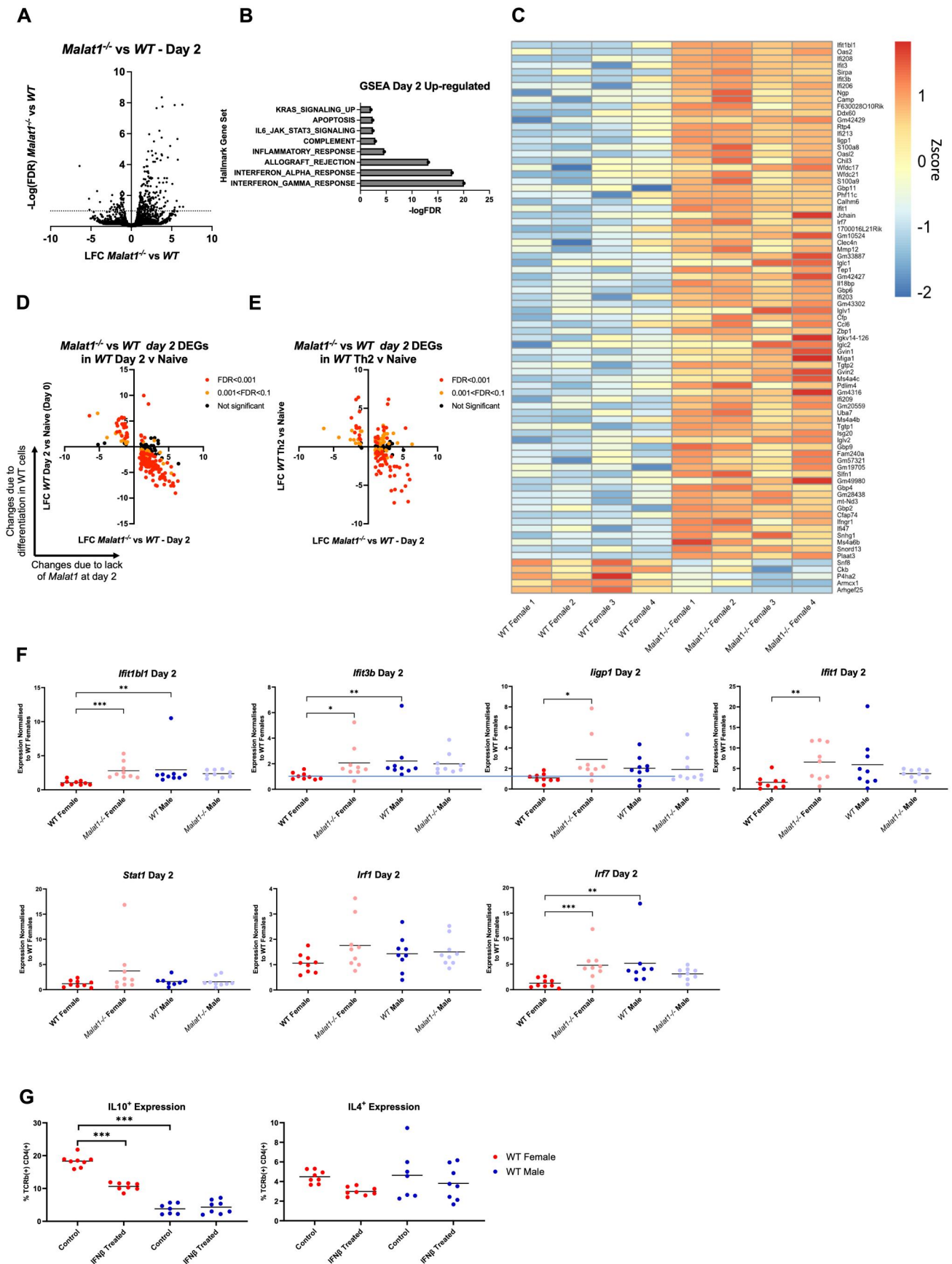


Figure 4. Impaired suppression of an IFN gene module during early differentiation of female *Malat1*^{-/-} Th2 cells. (A) Volcano plot displaying LFC in gene expression between WT and *Malat1*^{-/-} female cells (determined by Nanopore long-read RNAseq, n = 4 per group) against -logFDR at day 2 of in vitro differentiation. (B) Gene set enrichment analysis (GSEA) hallmark gene set terms enriched within significantly upregulated genes in *Malat1*^{-/-} cells at day 2 of in vitro differentiation. (C) Heatmap displaying Z score of log₂CPM for top DEGs (FDR < 0.01) between WT and *Malat1*^{-/-} cells at day 2 of

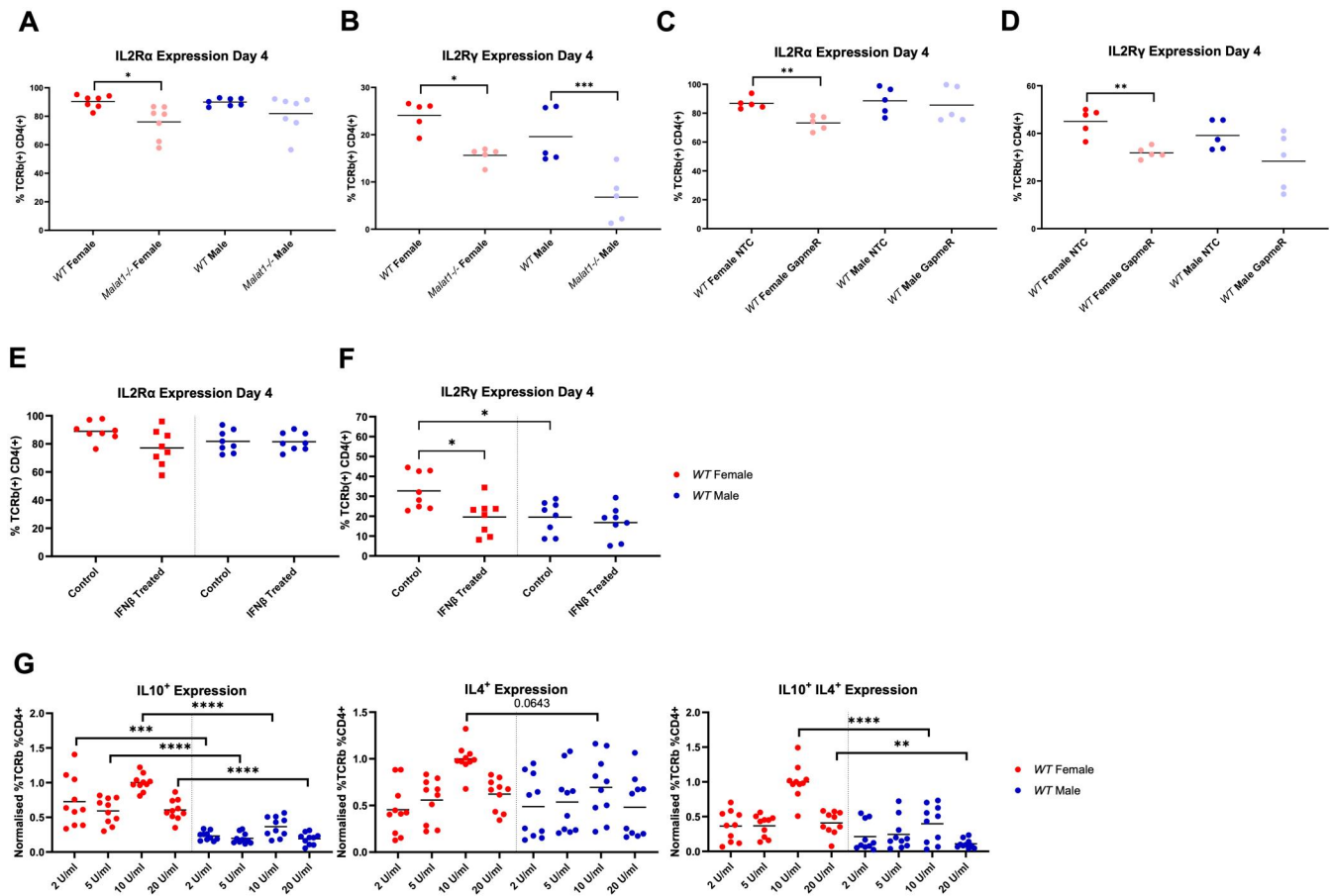


Figure 5. *Malat1* loss decreases expression of the IL-2 receptor and impairs the response to exogenous levels of IL-2 in cells from female mice. (A) Percentage of IL2Rα⁺ live TCRβ⁺ CD4⁺ WT or *Malat1*^{-/-} cells derived from female or male mice at day 4 of differentiation (levels determined by surface staining, n = 6). (B) Percentage of IL2Rγ⁺ live TCRβ⁺ CD4⁺ WT or *Malat1*^{-/-} cells derived from female or male mice at day 4 of differentiation (levels determined by surface staining, n = 5). (C) Percentage of IL2Rα⁺ live TCRβ⁺ CD4⁺ WT cells derived from female and male mice at day 4 of differentiation that were treated with either nontargeting control (NTC) or *Malat1* targeting GagneRs. Levels determined by surface staining (n = 5). (D) As in panel C, but for IL2Rγ⁺ live TCRβ⁺ CD4⁺ cells. (E) Percentage of IL2Rα⁺ live TCRβ⁺ CD4⁺ WT cells derived from female and male mice at day 4 of differentiation, treated with 0 (control) or 5,000 U/mL IFNβ. Levels determined by surface staining (n = 8). (F) As in panel E, but for IL2Rγ⁺. (G) Normalized percentage of IL-10⁺, IL-4⁺ or IL-10⁺ IL-4⁺ live TCRβ⁺ CD4⁺ WT or *Malat1*^{-/-} in vitro differentiated Th2 cells derived from female and male mice at day 6, with resuspension at day 4 in the indicated concentrations of IL-2. Levels determined by intracellular staining, and normalized to average levels in WT female-derived cells treated with 10 U/mL IL-2 from each experiment (n = 10). **P* ≤ 0.05, ***P* ≤ 0.01, ****P* ≤ 0.001, *****P* ≤ 0.0001.

cellular infiltration in the lungs, including Th2 cells, and eosinophilia. Indeed, *S. mansoni* egg injection resulted in increased in lung cell numbers, although we note that this only reached statistical significance in WT female mice and *Malat1*^{-/-} male mice (Figs. S9 and S10A). Similar splenic cell numbers were observed under all conditions (Fig. S10B) and similar lung eosinophil numbers and activation, measured by RELMα expression (Fig. S10C, D). Notably, both lung and splenic CD4⁺ T cells in egg-injected female *Malat1*^{-/-} mice expressed lower levels of IL-10 than WT mice (Fig. 6B–D). IL-4⁺/IL-10⁺ cells were also decreased in the lungs (percentage) and spleens (percentage and numbers) of egg-injected *Malat1*^{-/-} mice (Fig. 6E, F). This was also the case for triple-positive IL-4⁺/IL-13⁺/IL-10⁺ Th2 cells in the lungs of egg-injected mice (Fig. S10E). None of these differences were observed when comparing male *Malat1*^{-/-} mice with WT controls. On the contrary, the percentage of splenic IL-4⁺/IL-10⁺ cells increased in egg-injected *Malat1*^{-/-} male mice. Under these conditions, we did not observe any differences in total IL-4 expression between egg-injected *Malat1*^{-/-} and WT female mice, although we noted an increase in IL-4-expressing splenic CD4⁺ T cells in male *Malat1*^{-/-} mice

compared with WT (Fig. S10F, G). IFNγ⁺ CD4⁺ T cells are also induced as a result of *S. mansoni* egg injection, and IL-10 levels were also reduced in female-specific manner within this population in the lungs of inflamed mice (Fig. S10H, I). With regard to activation status of CD4⁺ T cells, we observed a borderline nonsignificant decrease in activated (CD44^{high}/CD64L^{low}) lung CD4⁺ T cells in female *Malat1*^{-/-} mice compared with WT and no differences in the spleen (Fig. S10J, K). No differences were observed in percentage and activation status of myeloid cell populations in egg-injected mice (Fig. S10L, M). Overall, these results indicated that, as observed in our in vitro Th2 differentiation experiments, *Malat1* deficiency resulted in a female-specific impairment of Th2 cytokine expression, predominantly demonstrated by reduced IL-10 expression in Th2 cells.

Discussion

Understanding cell intrinsic mediators of sexual dimorphism in lymphocytes is critical to addressing differences in incidence and severity of immunopathologies between females and males.^{1–4} We demonstrate that *Malat1*, one of the most

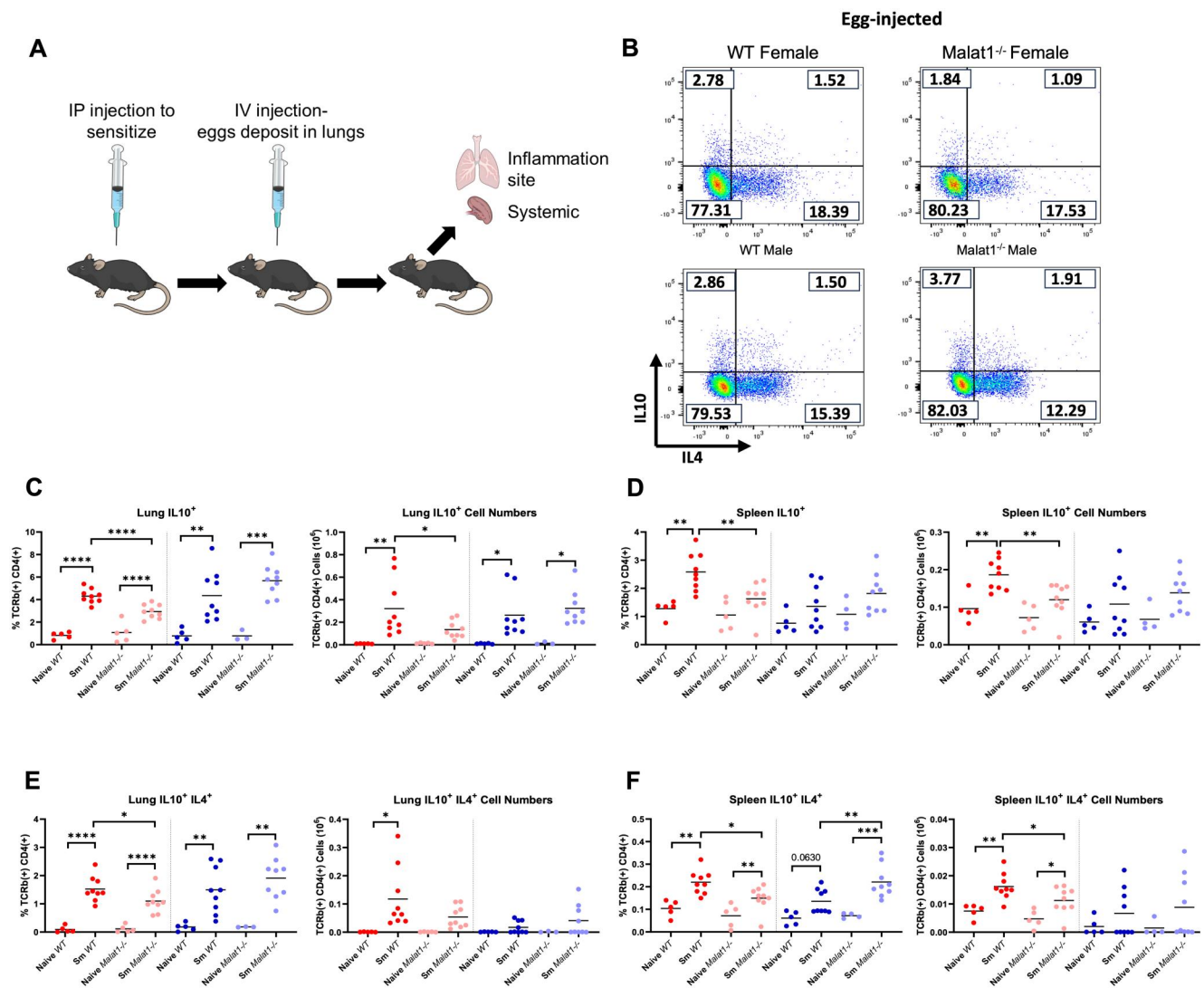


Figure 6. *Malat1* loss causes a female-specific decrease in Th2 cell-derived IL-10 levels in vivo. (A) Schematic of *S. mansoni* egg injection experiment. A total of 5,000 dead *S. mansoni* eggs were injected interperitoneally (IP) into mice, then after a week the injection was repeated intravenously (IV) via the tail vein. After another week, lungs and spleens were harvested and processed for FACS (art visuals from <https://bioart.niaid.nih.gov/>). (B) Representative FACS plots of IL-10 and IL-4 expression in lung CD4⁺ TCRb⁺ cells from *S. mansoni* egg-injected WT or *Malat1*^{-/-} female or male mice. (C) Percentage and cell numbers of lung IL-10⁺ TCRb⁺ CD4⁺ cells derived from naive or *S. mansoni* egg-injected WT or *Malat1*^{-/-} female and male mice. Levels determined by intracellular staining (n = 3 for *Malat1*^{-/-} male naives, n = 5 for all other naives, n = 9 for egg-injected mice). (D) As in panel C, but for splenic IL-10⁺ TCRb⁺ CD4⁺ cells (n = 4 for *Malat1*^{-/-} male naives, n = 5 for all other naives, n = 9 for egg-injected mice). (E) Percentage and cell numbers of lung IL-10⁺ IL-4⁺ TCRb⁺ CD4⁺ cells derived from naive or *S. mansoni* egg-injected WT or *Malat1*^{-/-} female and male mice. Levels determined by intracellular staining (n = 3 for *Malat1*^{-/-} male naives, n = 5 for all other naives, n = 9 for egg-injected mice). (F) As in panel E, but for splenic IL-10⁺ TCRb⁺ CD4⁺ cells (n = 4 for *Malat1*^{-/-} male naives, n = 5 for all other naives, n = 9 for egg-injected mice). *Sm*, *S. mansoni* egg injected. **P* ≤ 0.05, ***P* ≤ 0.01, ****P* ≤ 0.001, *****P* ≤ 0.0001.

highly abundant transcripts in mammalian cells, exerts a sex-specific function in Th2 differentiation, affecting early differentiation and endpoint cytokine expression in female cells, predominantly IL-10 (Fig. 7). *Malat1* deficiency has also some effects in male-derived cells, for example a modest suppression of early GATA3 expression and a suppression in IL2Rγ expression, yet these do not translate in changes in endpoint cytokine expression or gene expression program. Furthermore, the female-specific effect due to *Malat1* deficiency is observed in the *S. mansoni* egg injection model, as biological sex is a determinant of immune responses in the context of human schistosomiasis.³⁰ We also note that, although *Malat1* loss is associated with suppression of IL-10 both in vitro and in vivo, other effects of *Malat1* deficiency,

for example a modest suppression of IL-4, are only observed in vitro. This can be due to compensatory mechanisms and multiple effects contributing to cytokine expression in vivo. For example, through IL10R blockade we found in vitro that IL-4 and IL-13 levels in *Malat1*^{-/-} mice are likely to reflect both the loss of *Malat1* and reduced IL-10 levels from Th2 cells. This is in agreement with reports demonstrating that IL-10 suppresses activation of Th2 cells in vivo.³¹ We speculate that *Malat1* might play a critical role in Th2 differentiation in type 2 immunopathologies, especially those characterized by impaired IL-10 signalling.³² In addition, IL-10 has been shown to be expressed later than other effector cytokines³³ and from heterogeneous populations of CD4⁺ T cells.³⁴ As such, discrepancies between in vitro and in vivo

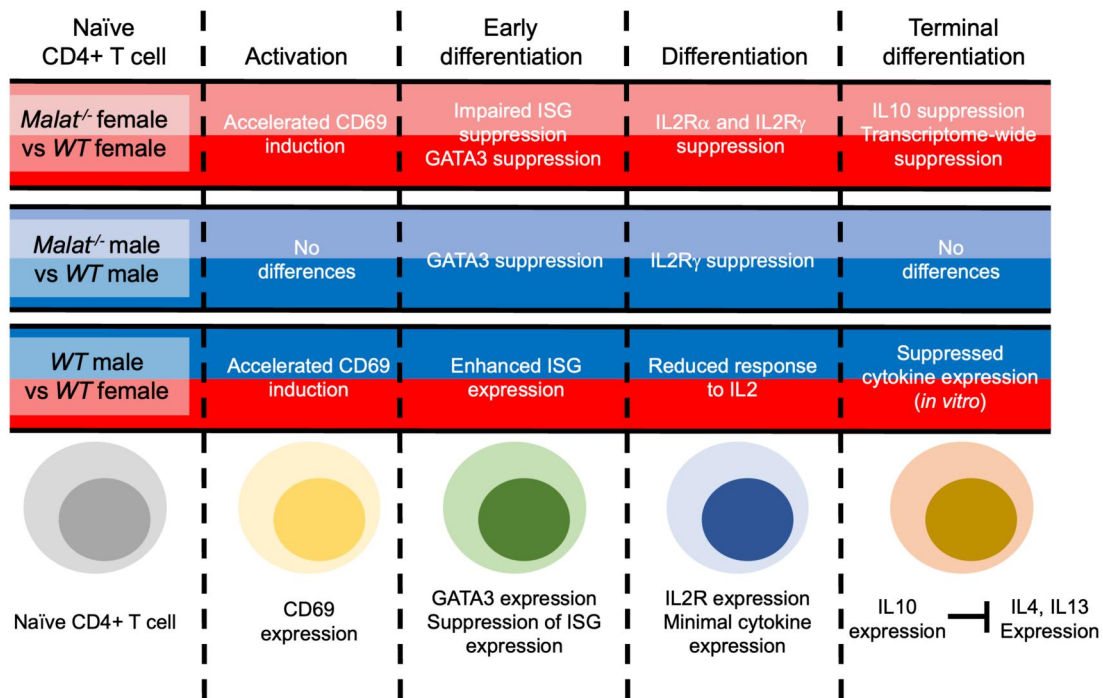


Figure 7. Schematic summary of the effect of *Malat1* loss on Th2 cell differentiation. The top row shows the effects observed when comparing *Malat1*^{-/-} female-derived cells with WT. The second row shows the comparison of male-derived *Malat1*^{-/-} and WT cells. The third row shows the comparison of male- and female-derived WT cells. Findings based on the in vitro process shown in Fig. 1A.

cytokine expression can be due to the time-point assessed and kinetics of Th2 cell emergence in the *S. mansoni* egg injection model. Nevertheless, the observed impairment of cytokine expression during in vitro Th2 differentiation and in the *S. mansoni* egg injection model strongly support a cell-intrinsic function of *Malat1* in controlling Th2 differentiation in a sex-specific manner.

Despite the limitation of not capturing the complexities of in vivo Th2 cell differentiation, in vitro differentiation of naïve CD4⁺ T cells to Th2 cells allowed us to demonstrate that *Malat1* loss results in a sex-specific impairment of differentiation in a cell-intrinsic manner. Mechanistically, downregulation of IL2R upon *Malat1* loss, prior to exposure to exogenous IL-2, results in a transcriptome-wide suppression of the Th2 differentiation program. Although downregulation of IL2R γ is observed in both male and female cells, IL2R α , which is necessary for formation of the high affinity IL2R, is only suppressed in female cells. In vitro, male Th2 differentiating cells are less responsive to IL-2 with regard to cytokine expression, providing an additional potential explanation of the sex specificity of the observed effect. Evidence for sexual dimorphism in response to IL-2 in other immune cell types has been already reported. Female (ILC2 (group 2 innate lymphoid) cells demonstrate increased proliferation in response to IL-2 when compared with male ILC2 cells,³⁶ and female natural killer cells produce higher levels of IFN γ than males in response to increased levels of IL-2.³⁷

We postulated that the observed downregulation of IL2R α and IL2R γ on day 4 is preceded by impaired early differentiation (days 2 to 3) of *Malat1*^{-/-} cells, an effect that is more pronounced in female cells. To probe how early *Malat1* deficiency impairs Th2 cytokine expression, we used long-read RNA sequencing as a superior method in identifying effects on gene expression and, particularly, splicing. *Malat1* deficiency had minimal effects on DTU at day 2

postdifferentiation induction. We did not analyze our end-point (day 6) short-read RNA sequencing experiments for DTU because¹ our data showed that it was the effect of *Malat1* on early Th2 differentiation that was driving the phenotype of *Malat1*^{-/-} Th2 cells (Figs. 2 and 3),² and any effects would most likely be a result of impaired response to IL-2 (Fig. 5) rather than a direct effect of *Malat1*. Indeed, rather than changes in splicing, we found that early differentiation of female *Malat1*^{-/-} cells is characterized by impaired suppression of an ISG cluster. It is notable that Th cells demonstrating ISG (including expression of *Ifit3*, *Irf7*, and *Stat1*, but not *Ifng*) have been described in type 2 inflammation both in humans³⁸ and in mouse models.³⁹ In all cases, these Th cells represent a distinct population to Th2 cells indicating that this signature needs to be suppressed in Th2 cells, which is in agreement with our findings in WT cells. Interestingly a recent publication identified an IFN-experienced population of naïve CD4⁺ T cells that show impaired response to TCR stimulation, as seen here for *Malat1*^{-/-} cells.⁴⁰ Another report demonstrated that these cells exist constitutively including in germ free mice.⁴¹ The 50-gene signature that defines IFN-experienced naïve CD4⁺ T cells⁴⁰ displays substantial overlap with the *Malat1*-regulated gene cluster (at day 2) identified here (26/50 genes, including *Irf7* and *Stat1*). Taken together with the observed effect of IFN β on Th2 differentiation here (partially phenocopying of *Malat1* deficiency), this suggests that suppression of this ISG signature in naïve CD4⁺ T cells is necessary for optimal Th2 differentiation and regulated by *Malat1* in female-derived cells. Of note, sexual dimorphism in IFN responses and ISG expression have been reported.^{42,43} It will be interesting to further investigate how *Malat1* promotes specifically downregulation of ISGs in female cells during early CD4⁺ T cell differentiation. It has been shown that *Malat1* can promote gene set-specific Polycomb Repressor Complex-mediated epigenetic silencing

in CD8⁺ T cells.²⁴ It could be explored whether this is also the case for ISGs in naive CD4⁺ T cells.

Our results suggest that the impairment of early Th2 differentiation in female *Malat1*^{-/-} cells is associated with a stronger but shorter-lived initial activation (0–24 h), as measured by CD69 expression. Indeed, strong T cell receptor stimulation in the presence of CD28 costimulation has been previously linked to impaired Th2 differentiation.⁴⁴ During the first 24 h of activation, male WT cells demonstrate CD69 expression kinetics similar to female *Malat1*^{-/-} cells, while deletion of *Malat1* does not cause any further increase in CD69 expression in male cells. Overall, we propose that *Malat1* downregulation upon activation of naïve CD4⁺ T cells facilitates activation, potentially through release of associated proteins that contribute cotranscriptional processing. However, in female cells, complete loss of *Malat1* alters activation kinetics, which in combination with failure to suppress expression of ISGs, leads to impaired Th2 differentiation and subsequent suppression of IL2R and IL-2-mediated cytokine expression. Male cells are not sensitive to *Malat1* loss, at least partly, due to their higher early activation threshold, higher ISG expression during early differentiation, and lower sensitivity to exogenous IL-2 during the later stages of differentiation.

We cannot exclude additional female-specific mechanisms being affected by *Malat1*, for example with regard to regulation of X chromosome-linked genes and the role of X chromosome inactivation during Th2 differentiation.¹⁰ Furthermore, it will be essential for our results to be validated in other models of type 2 immunity and in human CD4⁺ T cells. Despite these limitations, our study reveals that female Th2 cells show a specific dependence on *Malat1*, a highly expressed lincRNA not located on a sex chromosome and displaying similar expression in male and female CD4⁺ T cells. This can have far-reaching implications for our understanding of immune sexual dimorphism and provide novel routes for sex-specific manipulation of adaptive immunity.

Acknowledgements

The authors thank Sally James and Fabiano Pais at the Genomics Lab and Data Science Hub, respectively, in the University of York Bioscience Technology Facility for support with long-read sequencing data. They thank Joanna Greenman for technical support and Allison Green for comments on the paper.

Author contributions

M.G. (Formal analysis [Lead], Investigation [Lead], Methodology [Lead], Validation [Lead], Writing—original draft [Equal], Writing—review & editing [Equal]), K.A.W. (Data curation [Equal], Formal analysis [Equal], Investigation [Equal], Methodology [Equal], Project administration [Equal], Validation [Equal], Writing—review & editing [Equal]), S.V.D. (Formal analysis [Supporting], Writing—review & editing [Supporting]), I.K. (Supervision [Supporting], Writing—review & editing [Supporting]), D.C. (Supervision [Supporting], Writing—review & editing [Supporting]), S.A.T. (Funding acquisition [Supporting], Supervision [Supporting], Writing—review & editing [Supporting]), K.R.J. (Data curation [Equal], Formal analysis [Equal], Resources [Equal], Writing—review & editing [Supporting]), J.H. (Formal analysis [Supporting], Funding acquisition [Supporting], Investigation [Supporting],

Methodology [Supporting], Writing—review & editing [Equal]), D.L. (Conceptualization [Lead], Data curation [Supporting], Formal analysis [Supporting], Funding acquisition [Lead], Project administration [Lead], Resources [Lead], Supervision [Equal], Writing—original draft [Lead], Writing—review & editing [Lead]).

Supplementary material

Supplementary material is available at *The Journal of Immunology* online.

Funding

This work was funded by the Hull York Medical School (PhD studentship to M.G. and additional funding to D.L.), the Biotechnology and Biological Sciences Research Council White Rose doctoral training partnership (to K.A.W., reference BB/J014443/1), and the Medical Research Council (to J. P.H., reference MR/W018578/1).

Conflicts of interest

S.A.T. has served as a scientific advisory board member of ForeSite Labs, OMass Therapeutics, Qiagen, and Xaira Therapeutics; is a co-founder and equity holder of TransitionBio and Ensocell Therapeutics; is a nonexecutive director of 10x Genomics; and is a part-time employee of GlaxoSmithKline. All other authors have no financial conflicts of interest.

Data availability

Raw data are available upon request. RNAseq data have been deposited in the National Center for Biotechnology Gene Expression Omnibus database at <https://www.ncbi.nlm.nih.gov/geo/>. Accession numbers are GSE279185 for Illumina RNAseq and GSE278413 for Oxford Nanopore Technologies RNAseq data.

References

1. Gal-Oz ST et al. ImmGen report: sexual dimorphism in the immune system transcriptome. *Nat Commun* 2019;10:4295.
2. Klein SL, Flanagan KL. Sex differences in immune responses. *Nat Rev Immunol.* 2016;16:626–638.
3. Marquez EJ et al. Sexual-dimorphism in human immune system aging. *Nat Commun* 2020;11:751.
4. Takahashi T, Iwasaki A. Sex differences in immune responses. *Science.* 2021;371:347–348.
5. Dodd KC, Menon M. Sex bias in lymphocytes: Implications for autoimmune diseases. *Front Immunol.* 2022;13:945762.
6. Rubtsova K, Marrack P, Rubtsov AV. Sexual dimorphism in autoimmunity. *J Clin Invest.* 2015;125:2187–2193.
7. Whitacre CC, Reingold SC, O'Looney PA. A gender gap in autoimmunity. *Science.* 1999;283:1277–1278.
8. Shepherd R, Cheung AS, Pang K, Saffery R, Novakovic B. Sexual dimorphism in innate immunity: the role of sex hormones and epigenetics. *Front Immunol.* 2020;11:604000.
9. Lambert KC et al. Estrogen receptor alpha (ERalpha) deficiency in macrophages results in increased stimulation of CD4+ T cells while 17beta-estradiol acts through ERalpha to increase IL-4 and GATA-3 expression in CD4+ T cells independent of antigen presentation. *J Immunol.* 2005;175:5716–5723.
10. Syrett CM et al. Altered X-chromosome inactivation in T cells may promote sex-biased autoimmune diseases. *JCI Insight.* 2019;4.

11. Dou DR et al. Xist ribonucleoproteins promote female sex-biased autoimmunity. *Cell*. 2024;187:733–749.e16.
12. Engreitz JM, Ollikainen N, Guttman M. Long non-coding RNAs: spatial amplifiers that control nuclear structure and gene expression. *Nat Rev Mol Cell Biol*. 2016;17:756–770.
13. Gutschner T et al. The noncoding RNA MALAT1 is a critical regulator of the metastasis phenotype of lung cancer cells. *Cancer Res*. 2013;73:1180–1189.
14. Tripathi V et al. The nuclear-retained noncoding RNA MALAT1 regulates alternative splicing by modulating SR splicing factor phosphorylation. *Mol Cell*. 2010;39:925–938.
15. Lamond AI, Spector DL. Nuclear speckles: a model for nuclear organelles. *Nat Rev Mol Cell Biol*. 2003;4:605–612.
16. Tripathi V et al. Long noncoding RNA MALAT1 controls cell cycle progression by regulating the expression of oncogenic transcription factor B-MYB. *PLoS Genet*. 2013;9:e1003368.
17. Eißmann M et al. Loss of the abundant nuclear non-coding RNA MALAT1 is compatible with life and development. *RNA Biol*. 2012;9:1076–1087.
18. Nakagawa S et al. Malat1 is not an essential component of nuclear speckles in mice. *RNA*. 2012;18:1487–1499.
19. Zhang B et al. The lncRNA Malat1 is dispensable for mouse development but its transcription plays a cis-regulatory role in the adult. *Cell Rep*. 2012;2:111–123.
20. Hewitson JP et al. Malat1 suppresses immunity to infection through promoting expression of Maf and IL-10 in Th cells. *J Immunol*. 2020;204:2949–2960.
21. Dey S et al. Downregulation of MALAT1 is a hallmark of tissue and peripheral proliferative T cells in COVID-19. *Clin Exp Immunol*. 2023;212:262–275.
22. Masoumi F et al. Malat1 long noncoding RNA regulates inflammation and leukocyte differentiation in experimental autoimmune encephalomyelitis. *J Neuroimmunol*. 2019;328:50–59.
23. Xue Y et al. Knockdown of lncRNA MALAT1 alleviates coxsackievirus B3-induced acute viral myocarditis in mice via inhibiting Th17 cells differentiation. *Inflammation*. 2022;45:1186–1198.
24. Kanbar JN et al. The long noncoding RNA Malat1 regulates CD8+ T cell differentiation by mediating epigenetic repression. *J Exp Med*. 2022;219:e20211756.
25. Saraiva M, O'Garra A. The regulation of IL-10 production by immune cells. *Nat Rev Immunol*. 2010;10:170–181.
26. Kaplan MH, Whitfield JR, Boros DL, Grusby MJ. Th2 cells are required for the *Schistosoma mansoni* egg-induced granulomatous response. *J Immunol*. 1998;160:1850–1856.
27. Sabin EA, Kopf MA, Pearce EJ. *Schistosoma mansoni* egg-induced early IL-4 production is dependent upon IL-5 and eosinophils. *J Exp Med*. 1996;184:1871–1878.
28. Percie Du Sert N et al. Reporting animal research: explanation and elaboration for the ARRIVE guidelines 2.0. *PLoS Biol*. 2020;18:e3000411.
29. Subramanian A et al. Gene set enrichment analysis: a knowledge-based approach for interpreting genome-wide expression profiles. *Proc Natl Acad Sci U S A*. 2005;102:15545–15550.
30. Eloi-Santos S, Olsen NJ, Correa-Oliveira R, Colley DG. *Schistosoma mansoni*: mortality, pathophysiology, and susceptibility differences in male and female mice. *Exp Parasitol*. 1992;75:168–175.
31. Coomes SM et al. CD4(+) Th2 cells are directly regulated by IL-10 during allergic airway inflammation. *Mucosal Immunol*. 2017;10:150–161.
32. Hawrylowicz CM, O'Garra A. Potential role of interleukin-10-secreting regulatory T cells in allergy and asthma. *Nat Rev Immunol*. 2005;5:271–283.
33. Yssel H et al. IL-10 is produced by subsets of human CD4+ T cell clones and peripheral blood T cells. *J Immunol*. 1992;149:2378–2384.
34. Brockmann L et al. Molecular and functional heterogeneity of IL-10-producing CD4(+) T cells. *Nat Commun*. 2018;9:5457.
35. Shouse AN, LaPorte KM, Malek TR. Interleukin-2 signaling in the regulation of T cell biology in autoimmunity and cancer. *Immunity*. 2024;57:414–428.
36. Cephus JY Jr, et al. Testosterone attenuates group 2 innate lymphoid cell-mediated airway inflammation. *Cell Rep*. 2017;21:2487–2499.
37. Menees KB et al. Sex- and age-dependent alterations of splenic immune cell profile and NK cell phenotypes and function in C57BL/6J mice. *Immun Ageing*. 2021;18:3.
38. Seumois G et al. Single-cell transcriptomic analysis of allergen-specific T cells in allergy and asthma. *Sci Immunol*. 2020;5:eaba6087.
39. Tibbitt CA et al. Single-cell RNA sequencing of the T helper cell response to house dust mites defines a distinct gene expression signature in airway Th2 cells. *Immunity*. 2019;51:169–184.e5.
40. Deep D et al. Correction: precursor central memory versus effector cell fate and naive CD4+ T cell heterogeneity. *J Exp Med*. 2024;221:e2023119310182024c.
41. Even Z et al. The amalgam of naive CD4(+) T cell transcriptional states is reconfigured by helminth infection to dampen the amplitude of the immune response. *Immunity*. 2024;57:1893–1907.e6.
42. Gal-Oz ST, et al.; Immunological Genome Project. Microheterogeneity in the kinetics and sex-specific response to type I IFN. *J Immunol*. 2024;213:96–104.
43. Pujantell M, Altfeld M. Consequences of sex differences in type I IFN responses for the regulation of antiviral immunity. *Front Immunol*. 2022;13:986840.
44. Tao X, Constant S, Jorritsma P, Bottomly K. Strength of TCR signal determines the costimulatory requirements for Th1 and Th2 CD4+ T cell differentiation. *J Immunol*. 1997;159:5956–5963.